QUARTERLY OF APPLIED MATHEMATICS

Vol. XIX OCTOBER, 1961 No. 3

ON THE ONE-DIMENSIONAL FLOW OF A CONDUCTING GAS IN CROSSED FIELDS*

By

ERLING DAHLBERG

Department of Electronics, Royal Institute of Technology

and

Swedish State Power Board

Stockholm, Sweden

Abstract. The equations governing the quasi-one-dimensional steady flow of a conducting perfect gas in crossed, transverse electric and magnetic fields are treated under the assumptions that the electric conductivity is a scalar, that the wall drag is small and that the magnetic field due to the currents in the gas is negligible. The equations are normalized and different flow situations are illustrated by means of phase diagrams (drawn for a gas of constant specific heats, $\gamma = 1.33$). The possibility of a smooth transition from supersonic to subsonic motion is pointed out and the phenomena of standing shock fronts and choking are surveyed for constant-area, small-friction, power-yielding flow. The appendix contains some general remarks on the system of non-linear differential equations: $x' = P(x, y)/R(x, y)$; $y' = Q(x, y)/R(x, y)$.

Basic equations. We postulate steady flow of an (almost) inviscid fluid in a structure somewhat like the one outlined in Fig. 1. We assume that we have local thermodynamic equilibrium everywhere, that the fluid is a perfect gas, which may or may not have constant specific heats in the temperature range considered, that there exists a scalar electric conductivity and that heat flow and radiation, gravitation and boundary effects, except wall drag, may be neglected. We assume that wall friction is small and can be taken into account by employing the conventional gas-dynamic drag coefficient for

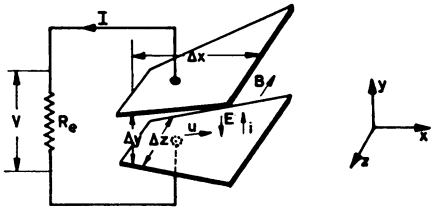

FIG. 1. *Outline of flow structure.* The conducting gas flows in the channel between the two electrodes and two insulating side walls (not shown). The gas velocity, u, and the electric field between the electrodes, E, are perpendicular to each other and to the magnetic field, B. If $u > E/B$, an induced current, I, will flow through the external load, R_e; if $u < E/B$, R_e should be replaced by a supply voltage, V, and the current should flow in the opposite direction, producing an accelerating volume force, iB, on the gas.

*Received December 1, 1960.

one-dimensional flow. We also assume that the magnetic field due to the currents in the gas is negligible and that, averaging over the cross section of the duct, we may neglect second-order terms in the variations from the mean values.

With positive directions according to Fig. 1, we then obtain the following three groups of equations

a) Gas relations

The equation of state $p/\rho = RT$

The specific heat $c_p = dh/dT = R\beta, \qquad \beta = \beta(T)$

For β = const. the enthalpy is $h = \beta p/\rho$

and the entropy is $s = R \ln (h^\beta/p)$

The Mach number $M = |u| (\beta p/(\beta - 1)\rho)^{-1/2}$

b) Electrical relations

The total current $I = \int_0^{\Delta x} (\Delta z) i \, dx$

Ohm's law, external circuit $V = E \, \Delta y = IR_e$

Ohm's law for the fluid $i = \sigma(uB - E)$

c) Mechanical relations

Conservation of mass $\rho u S = \text{const.}$

Conservation of momentum $\rho u S \, du/dx = -iBS - S \, dp/dx - F$

Conservation of energy $\rho u S \, d(h + u^2/2)/dx = -iES$

where iES is the electric power yield per unit length. Across a discontinuity (shock front) we must have

$$\begin{cases} \rho u = \text{const.} \\ p + \rho u^2 = \text{const.} \\ h + u^2/2 = \text{const.} \end{cases} \tag{1}$$

and, naturally, the entropy of the fluid may not decrease in passing the discontinuity.

Nomenclature

MKSA-units are used and the symbols have the following meanings

p	pressure	Δx, Δy, Δz	dimensions of apparatus
ρ	density	I	external current
R	gas constant (average)	V	external voltage
T	absolute temperature	R_e	external resistance
h	enthalpy per unit mass	i	current density
s	entropy per unit mass	σ	electric conductivity
β	normalized specific heat at constant pressure	B	magnetic field
		E	electric field
u	gas velocity	S	cross-section area
M	Mach number	F	wall drag per unit length

Principally the same equations have been treated by various authors using different simplifying assumptions to render them analytically tractable. Thus Way [7] has analysed, with numerical examples for power generators, three cases of frictionless constant-conductivity flow in constant electric and magnetic fields. These assumptions, obviously, do not yield a fully determined problem; thus Way introduces one of three restrictions: constant velocity, constant area or constant pressure. Neuringer [3] has analysed the constant-area, constant-conductivity flow in constant electric and magnetic fields. Especially, he has derived equations giving the electric field corresponding to maximum power for given length, magnetic field and inlet values. He presents numerical solutions for a certain inlet Mach number, which qualitatively agree with what should be expected according to our phase diagrams. However, the asymptotic solution, corresponding to $u \approx E/B$ at the inlet, should not give a finite limiting length ($\delta_{\max.}$). Berner and Camac [1], when considering a space propulsion device, have studied frictionless, constant-conductivity flow in a channel where the cross section and magnetic field are constant (but where the electric field varies). As further restriction they choose either constant temperature or a certain constant ratio between applied and induced electric field ($E/uB = (\beta + 1)/2$), which they somewhat arbitrarily designate as the maximum acceleration case. This case has also been analysed by Resler and Sears [5]. Sutton [6] has made a study of frictionless flow in a constant magnetic field and with $E/uB = \frac{1}{2}$ (corresponding to a local matching of external and internal load, i.e. $iE = i^2/\sigma$). Generally, he assumes constant conductivity, and as further restriction he uses constant velocity (also for varying σ), constant temperature, constant pressure, constant density or a cross section of constant area but varying shape. The slightly different problem where the currents close in the gas has been analysed in connexion with two experiments by Patrick and Brogan [4]. Finally the constant-area flow with friction in constant electric and magnetic fields was studied by the present author in a preliminary report [2]. In all these reports the gas was taken to have constant specific heats.

Normalization of the problem. In the following we shall treat the problem in a certain normalized form, which will enable us to give a qualitative outline of the possible types of flow by means of phase diagrams. The normalized problem may also be preferable for numerical integration.

We denote by a and b two characteristic quantities of dimension length and velocity respectively

$$a = \rho u/B^2\sigma\beta_0$$

$$b = E/B$$

and let subscript 0 indicate some chosen constant values[1].

We introduce two dimensionless variables

$$u^* = u/b_0$$

$$p^* = \beta_0 p/\rho u b_0$$

and two dimensionless parameters: the channel divergence parameter

[1]The quantity β_0 appearing in the equations is unessential and may well be put equal to unity. To obtain conformity with the preliminary report [2], we shall, however, put $\beta_0 = \beta$ for a gas of constant specific heats.

$$\psi = \frac{a}{S}\frac{dS}{dx}$$

and the wall drag parameter

$$\varphi = \beta_0 a 2f/D \geq 0,$$

where f and D are the conventional gas-dynamic expressions for the drag coefficient and the hydraulic diameter, $F = \rho u^2 S 2f/D$. (See e.g., A. H. Shapiro, *Compressible fluid flow*, New York, 1953, Art. 6.2)

The differential equations for the normalized variables are found to be

$$a\frac{du^*}{dx} = \frac{\left(u^* - \frac{b}{b_0}\right)\left(u^* - \frac{1}{\beta_0}\frac{b}{b_0}\frac{\beta_0}{\beta}\right) + u^*(\varphi u^* - \psi p^*)}{p^* - (\beta_0 - \beta_0/\beta)u^*} \tag{2}$$

$$a\frac{dp^*}{dx} = -\frac{\left(u^* - \frac{b}{b_0}\right)\left(p^* + \frac{\beta_0}{\beta}u^* - \frac{b}{b_0}\frac{\beta_0}{\beta}\right) + \left(p^* + \frac{\beta_0}{\beta}u^*\right)(\varphi u^* - \psi p^*)}{p^* - (\beta_0 - \beta_0/\beta)u^*}. \tag{3}$$

The expressions for the main physical quantities are

$$RT = p^* u^* b_0^2/\beta_0$$

$$dh = \frac{\beta}{\beta_0} b_0^2\, d(p^*u^*), \qquad \beta = \beta(p^*u^*).$$

For β = const., $\qquad h = p^*u^*b_0^2\beta/\beta_0$

$$iES = \sigma E^2 S(u^* - b/b_0)b_0/b = \rho u S(u^* - b/b_0)bb_0/a\beta_0$$

the electric energy extracted from unit mass per unit length being

$$\frac{iES}{\rho u S} = -b_0^2\left(\frac{\beta}{\beta_0}\frac{d(p^*u^*)}{dx} + \frac{1}{2}\frac{du^{*2}}{dx}\right) = -\frac{d}{dx}\left(h + \frac{u^2}{2}\right), \tag{4}$$

$$M^2 = (\beta_0 - \beta_0/\beta)u^*/p^*.$$

For $\beta = \beta_0$, we also have

$$s = R \ln [(p^*u^*)^\beta/p^*] + R \ln S + \text{const.},$$

$$a\frac{ds}{dx} = R\frac{(u^* - b/b_0)^2 + \varphi u^{*2}}{p^*u^*},$$

$$\rho u = \beta p_s/b_0 p^*(1 + u^*/2p^*)^\beta,$$

where p is the isentropic stagnation pressure.

We note that the critical line (see Appendix) of the system of differential equations, Eqs. (2) and (3)

$$p^* = (\beta_0 - \beta_0/\beta)u^*$$

corresponds to

$$M^2 = 1 \quad \text{or} \quad u^2 = \beta p/(\beta - 1)\rho$$

and that the jump relations, Eqs. (1), give

$$\rho_1 u_1 = \rho_2 u_2 ,$$

$$(p_2^* - p_1^*)/(u_2^* - u_1^*) = -\beta_0 ,$$

$$\int_1^2 (\beta/\beta_0)\, d(p^* u^*) = -\tfrac{1}{2}(u_2^{*2} - u_1^{*2}),$$

where subscripts 1 and 2 denote the state on the upstream and the downstream side of the discontinuity respectively.

For β = const., the last relation may be replaced by

$$(p_2^* + p_1^*)/2 - (\beta_0 - \beta_0/\beta)(u_2^* + u_1^*)/2 = 0,$$

i.e. the jump is centered on the critical line.

Because of the second law of thermodynamics, jumps may occur only from supersonic to subsonic motion

$$p_1^* - (\beta_0 - \beta_0/\beta_1)u_1^* < 0 < p_2^* - (\beta_0 - \beta_0/\beta_2)u_2^* .$$

For $\beta = \beta_0$, the change in entropy proves to be

$$(s_2 - s_1) = 2R\beta \sum_{n=1}^{\infty} \frac{\Delta^{2n+1}}{2n+1} (\gamma^{2n} - 1),$$

where $\gamma = \beta/(\beta - 1)$ is the ratio of specific heats, and

$$\Delta = (p_2^* - p_1^*)/(p_2^* + p_1^*)\gamma$$

is a measure of the shock strength.

We also note that

$$(dp^*/dx)/(du^*/dx) \to -\beta_0 \quad \text{when} \quad M \to 1.$$

A search for singular points, characterized by

$$dp^*/dx = du^*/dx = 0$$

for the physically interesting cases (E, B and σ finite or zero) leads to the following results. Let

$$G = p^* - (\beta_0 - \beta_0/\beta)u^*.$$

Then

$$G(dp^*/dx) = G(du^*/dx) = 0$$

gives either

$$a) \quad (0 < (b/b_0)^2/a < \infty)$$

$$u^* = b/b_0$$

$$\frac{\psi}{a} p^* = \frac{\varphi}{a} \frac{b}{b_0}$$

and possibly some points on the line $G = 0$, which we shall call pseudo-singular points,

or

$$b) \quad ((b/b_0)^2/a = 0)$$

$$\frac{\psi}{a} p^* = \frac{\varphi + 1}{a} u^*.$$

Phase diagrams. Numerical integration of Eqs. (2) and (3) would now yield the path of the phase point in the p^*u^*-plane for any particular flow situation with given initial values, etc. Without further simplification, little general knowledge is gained and the advantage of the normalized treatment is rather dubious. Because of the explicit x-dependence of the right-hand members of Eqs. (2) and (3), the phase point trajectory through any given point is not unique. However, in some cases it may be justifiable to neglect this x-dependence and we can then construct a phase diagram with unique trajectories.

If, for instance, the ratio between width and height of the channel does not vary, i.e. $\Delta y/\Delta z = \text{const.}$, we can assume

$$ES^{1/2} = \text{const.}$$

$$BS^{1/2} = \text{const.}$$

and consequently

$$E/B = \text{const.}$$

$$B^2/\rho u = \text{const.}$$

Thus

$$a = a_0\sigma_0/\sigma$$

$$b = b_0$$

(except in case of degeneracy, where we may have $b = 0$ or $b = \infty$. If $b = b_0 < 0$, the physically relevant part of the phase diagram is the third quadrant, $p^* < 0$, $u^* < 0$. We shall, however, not discuss this case.)

If, further, the area variation is moderate it may be permissible to use mean values for φ/a and ψ/a, especially as φ and ψ will mostly have the character of perturbation parameters. Finally, *when computing φ and ψ*, we must either assume that the electric conductivity is constant or approximate it by some function of p^* and u^* only.

Let us assume that we may take the conductivity to be constant in this connection and also that the fluid may be treated as having constant specific heats ($\beta = \beta_0 = \text{const.}$).

First, we consider the degenerate case, where the conductivity or the applied electric field is zero, which means that the power yield is identically zero. Equations (2) and (3) are then reduced to

$$\frac{du^*}{dx} = \frac{u^*(u^*(\varphi + 1)/a - p^*\psi/a)}{p^* - (\beta - 1)u^*} \tag{2'}$$

$$\frac{dp^*}{dx} = -\frac{(p^* + u^*)(u^*(\varphi + 1)/a - p^*\psi/a)}{p^* - (\beta - 1)u^*}. \tag{3'}$$

Here, b_0 is an arbitrary constant and the relevant parameters, $(\varphi + 1)/a$ and ψ/a, are

finite. The equations can be integrated directly, using Eq. (4), which is reduced to

$$p^*u^* + u^{*2}/2 = \text{const.} \tag{4'}$$

(The integration constant may be put equal to unity because of the arbitrariness of b_0). Equation (4') gives the shape of the trajectories, which are all similar. Evidently, if $\psi/a = (\varphi + 1)/a = 0$, every point is an equilibrium point, i.e. all flow variables are independent of x. Other possibilities are illustrated in Fig. 2, where the direction of motion along the trajectories is indicated by arrows. All diagrams in this and the following figures have been constructed for $\beta = \beta_0 = 4$, corresponding to $\gamma = 1.33$.

A second degenerate case is characterized by finite conductivity and electric field but zero magnetic field. Equations (2) and (3) are now

$$\frac{du^*}{dx} = \frac{C + u^*(u^*\varphi/a - p^*\psi/a)}{p^* - (\beta - 1)u^*}, \tag{2''}$$

$$\frac{dp^*}{dx} = -\frac{\beta C + (p^* + u^*)(u^*\varphi/a - p^*\psi/a)}{p^* - (\beta - 1)u^*}, \tag{3''}$$

(where $C = \sigma E^2/\rho u b_0^2$ may be put equal to unity because of the arbitrariness of b_0). The possible types of phase diagram are given in Fig. 3.

Thirdly, we have collected in Fig. 4 the types of phase diagram that obtain when either or both of φ and ψ are so small as to be negligible. When both φ and ψ are zero (Fig. 4.a), an exact integral of Eqs. (2) and (3) can be found

$$p^*u^* + u^{*2}/2 - p^*/\beta - u^* = K = \text{const.} \tag{5}$$

or, solving for p^*,

$$p^* = \frac{K + u^* - u^{*2}/2}{u^* - 1/\beta}.$$

Substituting this in Eq. (2) with $\varphi = \psi = 0$ and integrating, we find

$$\int \frac{\sigma\, dx}{\sigma_0 a_0} = -\int \left[\frac{\beta - \frac{1}{2}}{u^* - 1} + \frac{\beta - \frac{1}{2} + K\beta^2}{(\beta - 1)^2}\left(\frac{1}{u^* - 1/\beta} - \frac{1}{u^* - 1} + \frac{1 - 1/\beta}{(u^* - 1/\beta)^2}\right)\right] du^*. \tag{6}$$

It is evident from Eqs. (2) and (3) that, for small values of φ and ψ, the phase diagram will be substantially unaffected except near $u^* = b/b_0 = 1$ (and, for $\psi \neq 0$, for large p^*-values combined with relatively small values of u^*). Thus, except in special cases, it may often prove convenient to use Eqs. (5) and (6) for a first approximation[2]. On the other hand, it is obvious that the degeneracy, manifested by the line of singular points in Fig. 4.a, is removed by the introduction of a finite value of φ or ψ, no matter how small.

Finally, when both φ and ψ are finite, the phase diagrams will be similar to those in Fig. 5. In this figure we have also included a sketch indicating what regions in

[2]In the earlier report [2] six diagrams are presented, which, for $\beta = 4$ and different values of K, give $(B^2/\rho u)\int \sigma\, dx$, $\beta RT/b^2$ and M as functions of $(h + u^2/2)/b^2$. The diagrams also give $(\rho u)_i b/\beta p_{s_i}$ as a function of $(h_i + u_i^2/2)/b^2$, where subscript i refers to the state at the duct inlet and p_s is the isentropic stagnation pressure.

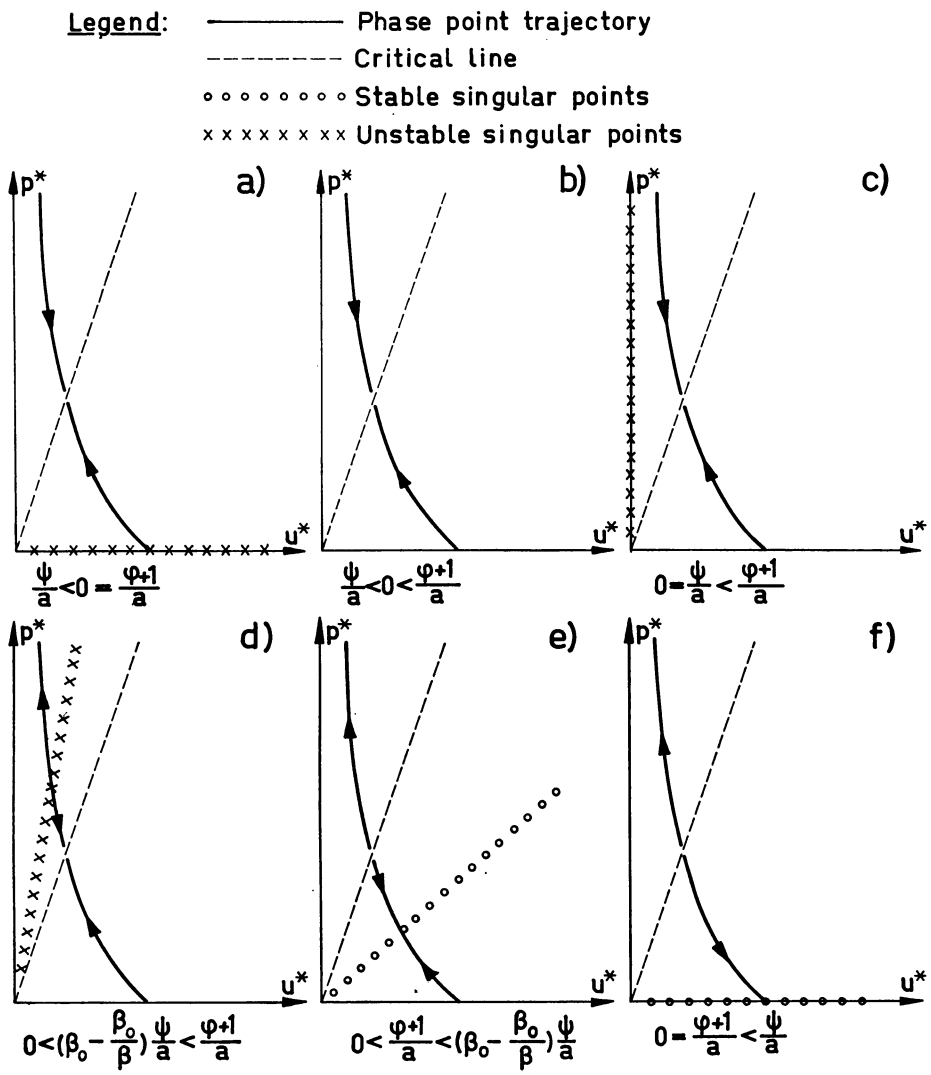

FIG. 2. *Phase diagrams for degenerate cases, I;* $\sigma E = O$. A phase diagram shows the variation along the channel of the normalized velocity, $u^* \propto u$, and the normalized pressure, $p^* \propto pS$, (where S is the cross-section area) for given values of the friction and channel divergence parameters, φ and ψ. In this figure we can recognize the normal gas-dynamic types of adiabatic flow. Thus, *a* represents frictionless convergent flow and *c* constant area flow friction; in both cases the gas velocity tends to approach the speed of sound, represented by the critical line. Further, *f* represents divergent frictionless flow, accelerated when supersonic and decelerated when subsonic. In *b* the effects of friction and area change (convergent) cooperate, whereas in *d* and *e* they oppose each other. The singular line in *d* and *e* corresponds to a balance between friction and area-change effects such that u^* and p^* are independent of x. With short-circuited electrodes ($E = 0$), the effect of the magnetic field, represented by $1/a$ in the parameter $(\varphi + 1)/a$, is analogous to that of friction.

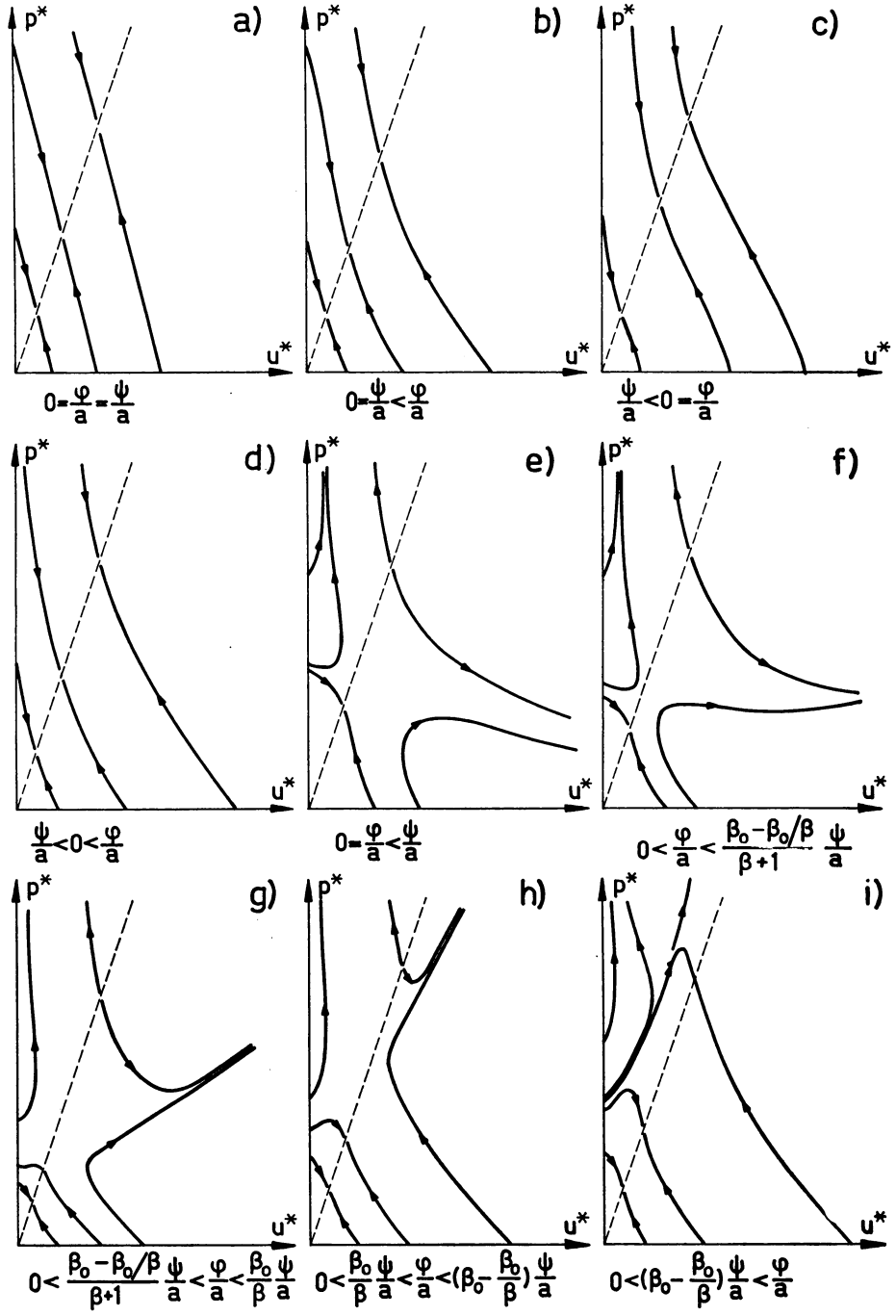

FIG. 3. *Phase diagrams for degenerate cases, II; B = O.* These diagrams illustrate the effect of Joule heating, σE^2, in the absence of magnetic forces. In *a* this is the only effect and we see that the velocity approaches the speed of sound. The effects of other factors—*b* friction, *c* convergent channel and *d* friction and convergent channel—which separately show the same tendency, will only modify the trajectories slightly. In *e* the effects of Joule heating and channel divergence oppose each other and we see that the former dominates at low pressures and velocities and the latter at high pressures and, less markedly, at high velocities. Friction, when small, will mainly influence the behaviour at low pressures and high velocities, *f*; its influence will gradually spread to higher pressures as the ratio between the friction and channel divergence parameters increases, *g*, *h* and *i*.

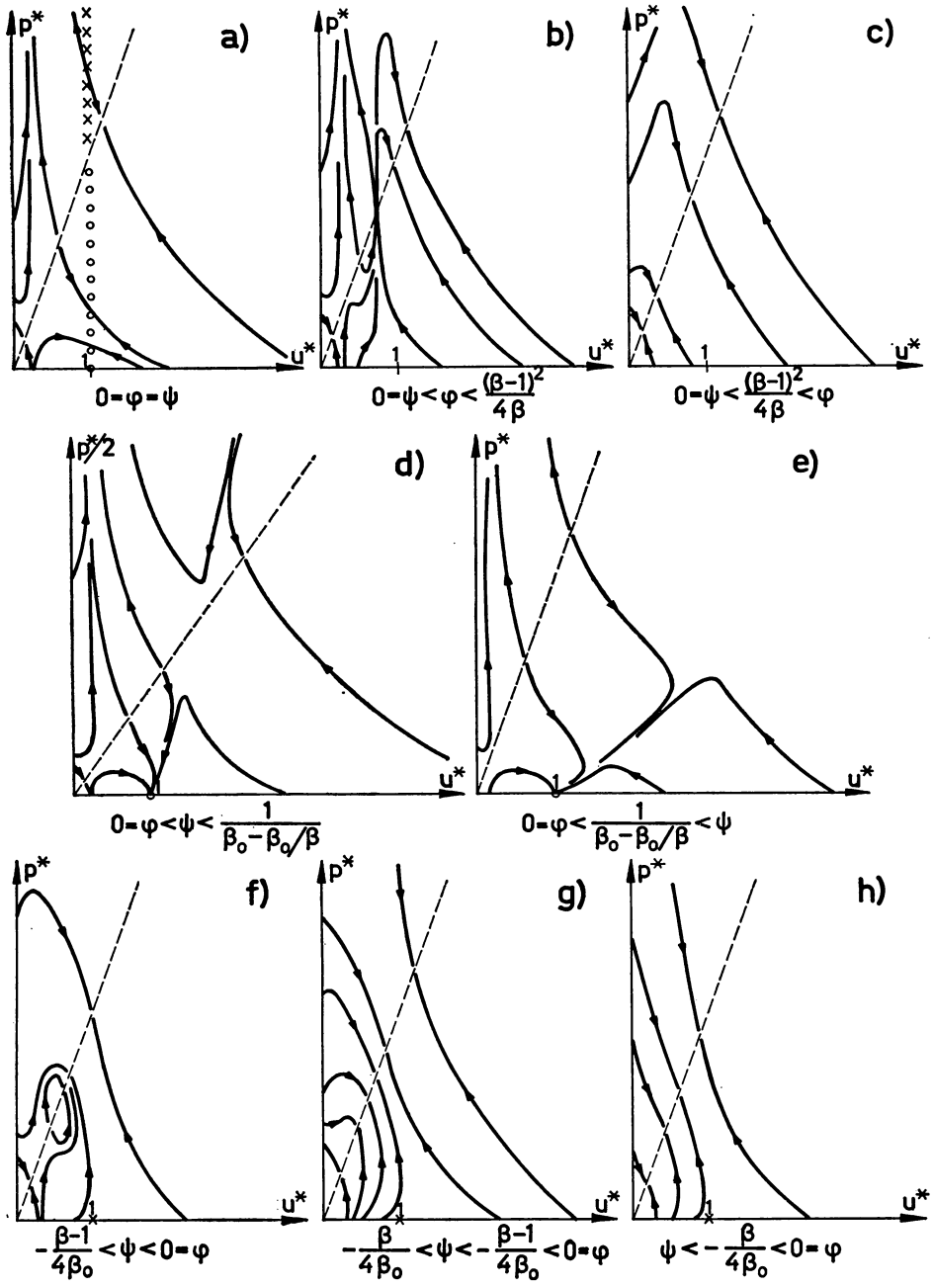

FIG. 4. *Phase diagrams*; $\varphi\ \psi = O$. (*N.B.* Contracted p^*-scale in *d*.) These diagrams represent the cases where friction and/or channel divergence are negligible. If these effects are small, the purely electromagnetic effects illustrated in *a* will dominate except near $u = E/B$ ($u^* = 1$). This may be seen from *b* (friction), *d* (divergent channel) and *f* (convergent channel). Near $u = E/B$ and when some other effect is great (*c*, *e*, *g* and *h*), the phase diagram will differ radically from *a*. One should note the smooth transition from supersonic to subsonic motion, which may occur with small friction, *b*, or small convergence (not shown).

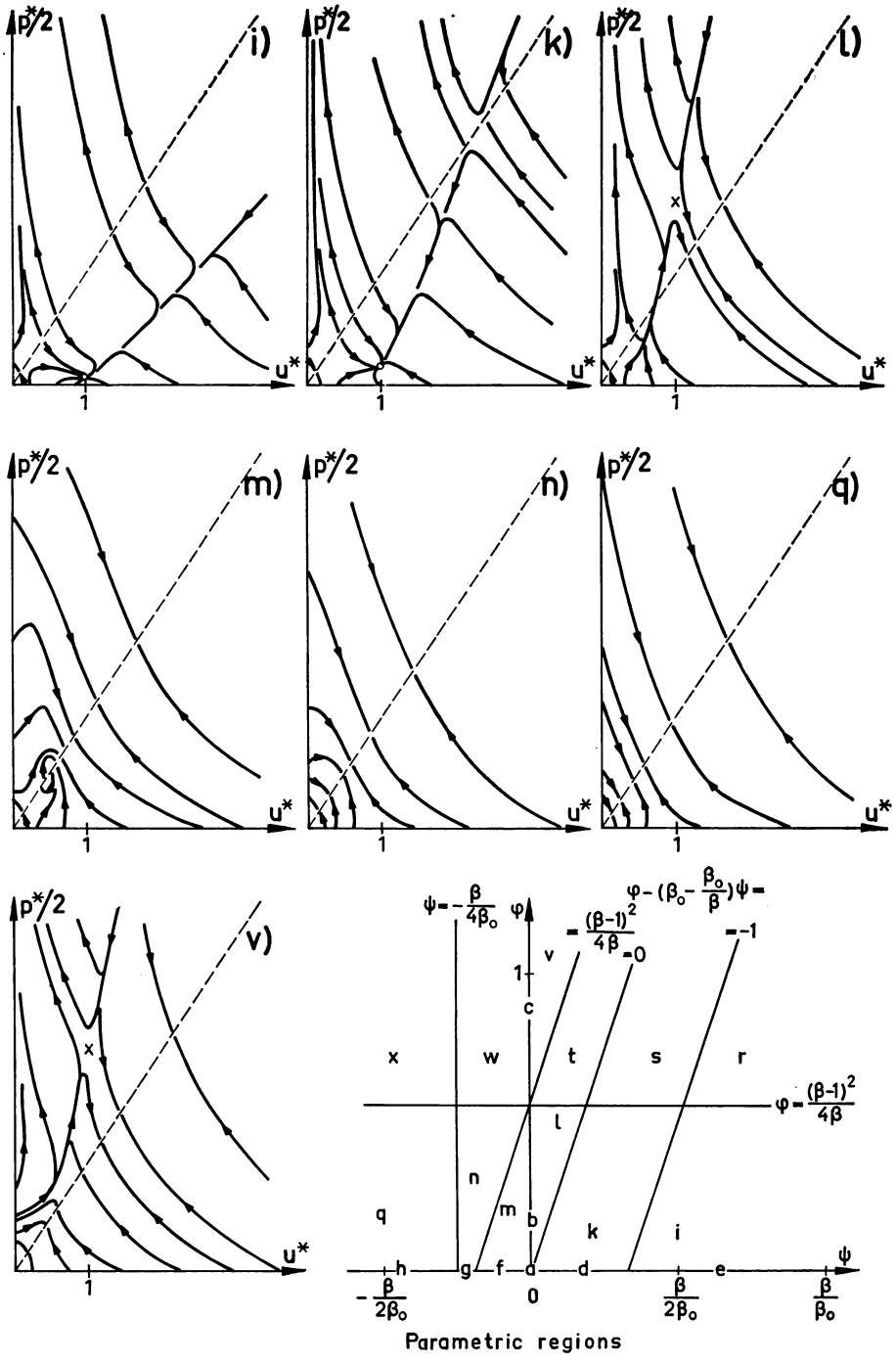

FIG. 5. *Phase diagrams;* $\varphi\ \psi \neq 0$. (*N.B.* Contracted p^*-scale.) These diagrams represent the cases where both friction and area change as well as electromagnetic effects must be taken into account. The values of φ and ψ for the different diagrams in this and the preceding figure are indicated by the letters in the map of parametric regions. In *i*, *k* (*r* and *s*) we note the existence of a stable equilibrium point for $u = E/B$ (u^* and p^* independent of x), in *l*, *v* (and *t*) it is unstable; this point corresponds to the singular line in Fig. 2, *d* and *e*. We also note the smooth transition from supersonic to subsonic motion that is characteristic for the regions *l*, *t* and a small part of region *m* (not illustrated).

the $\varphi\psi$-plane correspond to the various types of phase diagram illustrated; the letters refer to the phase diagrams in this and the preceding figure. (The regions r, s, t, w and x have not been illustrated; they differ from their respective lower neighbours i, k, l, n and q mainly in that the slope of the trajectories is negative along the whole u^*-axis.) We note that the singular point ($u^* = 1$, $p^* = \varphi/\psi$) is a stable nodal point in the supersonic range with no limit cycles for parameter values in regions i, k, r and s. When the parameters fall in the l, t or v regions, it is a saddle point in the subsonic range and, for $\psi < 0$, it falls outside the physically relevant part of the phase plane. Regarding the pseudo-singular points on the sonic line, we find that no such points exist for the parametric regions n, q, v, w and x; when they exist they are two in number, and the one nearest the origin is always in the first quadrant ($0 < u^* < 2/(\beta + 1)$) and is always a "saddle point". The one farthest from the origin may be a "saddle point" (in regions k and s, $u^* > 1$, and in regions i and r, $u^* < 0$), a "nodal point, stable from below," (in regions l and t and a small part of m near the φ-axis), a "focal point" (in the main part of region m) or a "nodal point, stable from above," (in a very small portion of region m near the bottom left hand corner); for all the latter cases we find $2/(\beta + 1) < u^* < 1$.

The pseudo-singular "nodal point" has a special significance in that the phase point moves across the critical line with a finite velocity, provided the initial point lies within a certain range. This implies the possibility of a continuous transition from supersonic to subsonic motion (or vice versa, depending on the type of "nodal point") without a throat in the duct and even when heat exchange effects are negligible. The parametric region where the pseudo-singular point is "nodal and stable from above" is, however, so narrow as virtually to exclude the possibility of a transition from subsonic to supersonic motion. (For $\beta = \beta_0 = 4$, the width of this region is, approximately,

$$-(\beta - 1)/4\beta < \psi < -(\beta - 1)/4\beta + 7\ 10^{-6}$$

for $\varphi = 0$ and decreases for increasing φ.) Further, the uniqueness of a trajectory disappears when it crosses the critical line at a pseudo-nodal point; thus the phase diagram does not tell what will happen downstream from a smooth transition, but it gives some indication as to what can happen. Physically, this may be determined by end conditions, but there might also exist a corresponding real indeterminacy.

In the general case, the phase point cannot cross the critical line except by discontinuous jumps from the supersonic to the subsonic range. This means that there may arise phenomena, somewhat analogous to the choking and the standing shock fronts known from compressible fluid flow in constant-area ducts with friction. (See e.g. Shapiro, *loc. cit.*) The analogy is far from perfect, however, as the electromagnetic "friction" force is negative for velocities smaller than E/B and also gives rise to energy exchange with the surroundings. A qualitative discussion of some typical cases of power-yielding, constant-area, small-friction flow, corresponding to the right-hand part of the phase diagram of Fig. 4.b, was given in the earlier report [2]. Keeping the boundary conditions fixed, we discussed how the phase-diagram image of the flow varies when the length of the electrode section (or, rather, the product of length and conductivity) is increased.

For a duct fed through a convergent nozzle and discharged into a constant-pressure receiver, we showed that the flow will gradually be choked and the exit velocity decrease until the velocity at the duct inlet corresponds to $u^* = 1$. When the length is increased further, the flow rate will remain almost constant and the exit velocity will

increase, as more and more energy is taken up by the gas from the external electric circuit. The existence of choking effects has been questioned by Neuringer [3] on the basis of his numerical results. Their absence there is, however, due to his assumption of constant inlet Mach number.

If the gas enters via a convergent-divergent nozzle and is let out into a low-pressure receiver, the (supersonic) exit velocity will first decrease while the inlet velocity remains constant. Provided that the trajectory lies above the range of smooth transition of the pseudo-nodal point, a shock front will develop at the outlet when the velocity there becomes sonic and, as the length is increased further, this shock front will move upstream. As long as $u^* > 1$ everywhere in the duct, the outlet velocity, while remaining sonic, will at first increase slightly because of friction effects, but, if the shock enters the nozzle, the (still sonic) outlet velocity will again decrease. The shock may reach the nozzle throat and vanish there; then the flow will be choked in analogy with the convergent nozzle case. Depending on the area ratio of the nozzle and the initial state of the gas, it may also happen, however, that the shock stops in the divergent part of the nozzle or in the electrode section. This implies that the velocity in the duct inlet or on the downstream side of the shock corresponds to $u^* \approx 1$ and, after this state has been reached, further increases in the length will not affect the flow upstream from this position, whereas the (sonic) outlet velocity will increase, as more and more energy is taken up by the gas from the external electric circuit.

If, however, the initial trajectory lies below the separatrix of the pseudo-nodal point—which, for small values of φ, is approximated by the no-friction trajectory through ($u^* = 1$, $p^* = \beta - 1$) with $K = (\beta - 2)(\beta - \frac{1}{2})/\beta$, Eq. (5)—no shock front should develop when the exit velocity becomes sonic[3]. Instead, the phase point should pass through the pseudo-nodal point with a finite velocity ($a\ dp^*/dx \approx \varphi/(\beta - 1)$). Beyond the pseudo-nodal point it will continue along that trajectory which makes the outlet velocity sonic. Thus, when the length is increased further, the phase point will follow successively higher-lying trajectories and the (sonic) outlet velocity increase, as more and more energy is taken up by the gas from the external electric circuit. That a smooth transition is the only physically plausible phenomenon in this case is evident, as a jump from a point on the (supersonic) trajectory should end to the left of the vertical line through the pseudo-nodal point, where the trajectories go to infinity, and it would be impossible to satisfy the end condition of sonic outlet velocity.

If the gas cannot be treated as having constant specific heats and/or constant conductivity, it is still feasible to construct a phase diagram for any given situation—provided that it is permissible to regard β and σ as functions of p^* and u^* only. In most cases it should be sufficient to take into account the temperature dependence ($T \propto p^*u^*$), but should it prove essential to include also a pressure dependence, it is necessary to disregard the area variation in this context by using $p \propto p^*/S \approx p^*/S_0$. We have not included any such phase diagrams, as they would appear as distorted images of those presented, lacking in generality and, qualitatively, without any significant new features.

Acknowledgments. I wish to thank Prof. H. Alfvén for his kind interest in the work, Dr. S. Lundquist and Prof. G. Borg for many helpful discussions and Mrs. K. Forsberg for drawing the figures.

[3]As the significance of the pseudo-singular points was not analysed in the preliminary report [2], this case was not included in the original survey and an erroneous statement was made (p. 14) to the effect that all trajectories in the region $u^* > 1$ end on the critical line.

References

1. F. Berner and M. Camac, *Air scooping vehicle*, AVCO Research Lab., Research Report 76, Aug. 1959
2. E. Dahlberg, *On magnetohydrodynamic generation of electric power*. I., Swedish State Power Board, P. M. A-34/60, April 1960
3. J. Neuringer, *Optimum power generation from a moving plasma*, J. Fluid Mech. **7**, 287–301 (1960)
4. R. M. Patrick and T. R. Brogan, *One-dimensional flow of an ionized gas through a magnetic field*, J. Fluid Mech. **5**, 289–309 (1959)
5. E. L. Resler & W. R. Sears, *The prospects for magneto-aerodynamics*, J. Aeronaut. Sci. **25**, 235–245 (1958) and *Ibid.* **26**, 318 (1959)
6. G. W. Sutton, *The quasi-one dimensional flow of an electrically conducting gas for the generation of electrical power*, General Electric Co. TIS Report R 59SD307, Feb. 1959
7. S. Way, *Design considerations in MHD generators*, Westinghouse Res. Lab., Scientific Paper 6-40509-2-Pl, Feb. 1960

Appendix

Remarks on a class of systems of non-linear differential equations. The system of non-linear differential equations studied in this report can be generalized as

$$\left.\begin{aligned} x' &= P(x, y)/R(x, y) \\ y' &= Q(x, y)/R(x, y) \end{aligned}\right\} (S_1)$$

(See e.g., Minorsky, *Non-linear mechanics*, Ann Arbor, 1947. Part IV. Chap. XX & XXII.) In addition to this system, we have the requirement—physically founded—that two functions, say $F(x, y)$ and $G(x, y)$, be continuous everywhere, whereas discontinuities in x and y may occur under certain, yet unspecified, circumstances.

The phase trajectories of S_1 are the same as those of

$$\left.\begin{aligned} x' &= P(x, y) \\ y' &= Q(x, y) \end{aligned}\right\} (S_2)$$

but the direction and magnitude of the phase point velocity may be different for the two systems. The topological methods for sketching the trajectories of S_2 are well-known and straightforward. (See e.g., Minorsky, *loc. cit.* Part I.) Let us assume that we have made an outline of the phase diagram of S_2 and that it includes the isoclines $P = 0$ and $Q = 0$, and, further, that we have found and sketched the isolated points and curves where $R = 0$. By studying the sign variation of P, Q and R, we can now find the direction of motion of the phase point along the trajectories in the regions bounded by the curves $P = 0$, $Q = 0$ and $R = 0$.

Before examining the behaviour of the solutions at non-normal points, we shall make a number of assumptions, which shall hold in the whole of (the relevant part of) the xy-plane.

A.1 F, G, P, Q and R are continuous.

A.2 The number of points where $P = Q = 0$ is finite. P and Q have continuous first derivatives at such points and $P_xQ_y - P_yQ_x$ does not vanish there.

A.3 $R = 0$ corresponds to a finite number of isolated points and a finite number of curves with a finite number of intersections. R possesses continuous first derivatives near points where $R = 0$ and continuous second derivatives, which do not all vanish, near points where $R = R_x = R_y = 0$.

A.4 P, Q, R, R_x and R_y do not vanish simultaneously.

A.5 At points where $R = 0$, the functions $F' = (F_x P + F_y Q)/R$ and $G' = (G_x P + G_y Q)/R$ exist and are continuous. This implies sufficient differentiability of the functions involved.

A.6 R, P, F_y and G_y do not vanish simultaneously.

A.7 R, Q, F_x and G_x do not vanish simultaneously.

We can now distinguish between four types of non-normal points of S_1 .

I. A *singular point* is a point where $P = Q = 0$ but $R \neq 0$. Its properties are similar to those of the corresponding point of S_2 , but its stability will depend on the sign of R.

II. A *critical point* is a point where $R = 0$ but neither both R_x and R_y nor both P and Q vanish. A line of such points is called a *critical line*. The phase point velocity along a trajectory through a critical point changes sign (and is infinite) at that point; thus, the phase point cannot proceed continuously through (or stop at) a critical point. The assumption commonly employed is that the phase point jumps discontinuously from the critical point to some other point determined by the continuity of F and G. In our case, the jump occurs before the phase point reaches the critical line; this type of jump is physically plausible when distance and not time is the independent variable and the end conditions can influence the state immediately behind the jump (e.g., subsonic motion after the discontinuity). An interesting property of critical (and pseudo-critical, see below) points is evident from the assumption (A.5). Denoting a unit vector parallel to the trajectory through the point by $\mathbf{s}$, we find

$$\mathbf{s} \cdot \operatorname{grad} F = \mathbf{s} \cdot \operatorname{grad} G = 0$$

which means that either $F(G)$ has a stationary value or grad F (grad G) is perpendicular to the trajectory. Should either of the gradients, say grad G, vanish at more than a finite number of points where $R = 0$, we may replace G by a suitable combination, such as $H = F + G$. Thus, normally the curves $F = \text{const.}$ and $G = \text{const.}$ ($H = \text{const.}$) are tangent to each other and to the trajectories at their intersection with curves corresponding to $R = 0$. If F or G is linear, say $F = y - kx$, $R = 0$ is obviously an isocline ($dy/dx = k$). We also see that jumps originating *at* critical points are impossible if no pair of curves, $F = \text{const.}$; $G = \text{const.}$, possesses more than two points of intersection.

III. A *pseudo-singular* (*pseudo-nodal, etc.*) *point* is a point where $P = Q = R = 0$ but R_x and R_y do not both vanish. Given the assumptions above, we can prove that *any intersection between* $R = 0$ *and* $P = 0$ *or between* $R = 0$ *and* $Q = 0$ *is a pseudo- singular point.* If we assume e.g., $R = P = 0$, the assumption (A.5) gives $F_y Q = G_y Q = 0$; and Q must vanish, as, according to (A.6), F_y and G_y do not both vanish. The phase point velocity at the point will depend on the slope of the trajectory; using (A.2) we find that it will differ from zero, and using (A.4) that it will be finite, except if the trajectory should happen to be parallel to the critical line. In Fig. 6 we have illustrated the different types of pseudo-singular points, corresponding to the three types of singular points.

a) Pseudo-focal (pseudo-vortex) point. The point is surrounded by arc-shaped trajectories beginning and ending on the critical line.

b) Pseudo-nodal point. This point—like an ordinary nodal point—can be characterized by two slopes: the "slope of approach" and the slope of the separatrix. We may expect a smooth transition if the phase point initially lies within the cross-hatched region. In a boundary-value problem like ours, the end condition may determine which trajectory the phase point will follow after passing the pseudo-nodal point; in an initial-

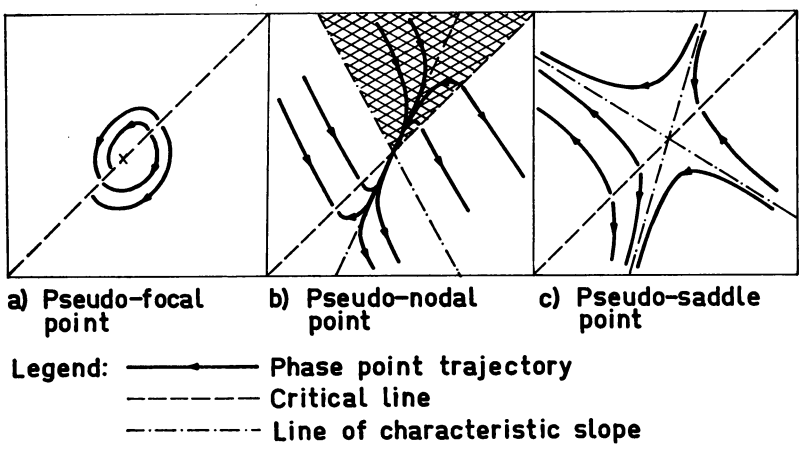

FIG. 6. *Pseudo-singular points.*

value problem this may be undetermined or determined by factors neglected in the analysis.

c) Pseudo-saddle point. This point is again characterized by two slopes, corresponding to the two separatrices separating the regions where the trajectories end on the critical line, turn back, and begin on the critical line respectively.

It is not to be expected that the separatrices, being discrete trajectories, correspond to physically observable smooth transitions. The application of restrictions having the nature of desiderata, such as constant gas velocity throughout the duct in our case, may easily hide the nature of the pseudo-singular point and lead to the presumably erroneous conclusion that a smooth transition will occur at a pseudo-saddle point (see e.g. Sutton [6]). If it should happen that the slope of the critical line equals one of the characteristic slopes, and especially the "slope of approach" of a pseudo-nodal point, further considerations may be necessary. One should, however, first of all ascertain that it does not depend on a never fully realizable desideratum, such as perfect symmetry of a circuit.

IV. A *pseudo-critical point* is a point where $R = R_x = R_y = 0$ but neither all of R_{xx}, R_{xy} and R_{yy} nor both P and Q vanish. It was proved above that $R = PQ = 0$ implies $R = P = Q = 0$; thus, neither P nor Q vanishes at a pseudo-critical point. Isolated points where $R = 0$ are pseudo-critical, as are points of intersection of critical lines; there may also exist lines of pseudo-critical points. Except in cases where the trajectory is parallel to a critical or pseudo-critical line, the phase point velocity along a trajectory through a pseudo-critical point, though becoming infinite at the point, does not change sign. The motion of the phase point is integrable and the pseudo-critical point will not affect the continuity of the solution. In contrast with the discrete trajectories leading through a pseudo-saddle point, the discrete continuous trajectory leading through the pseudo-critical point at the intersection of two critical lines may well have a physically observable counterpart. The motion of the phase point along a trajectory near that through the pseudo-critical point should, in general, be quasi-continuous, i.e. when it reaches the first critical line the phase point will jump to a point on the same (S_2)-trajectory beyond the second critical line (Fig. 7a). To prove this we assume that $F_0' \neq 0$

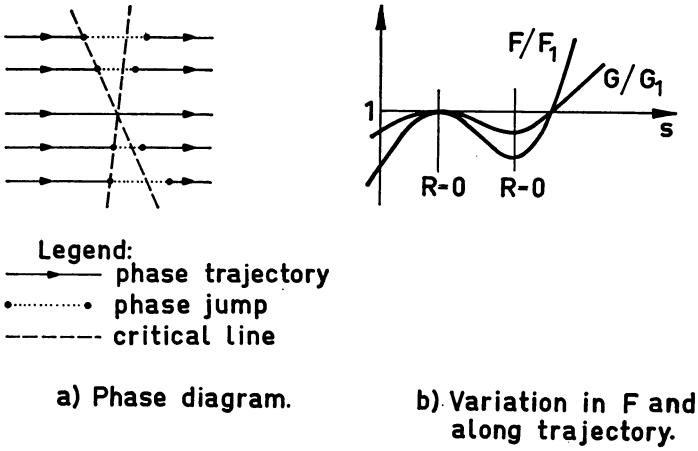

FIG. 7. *Intersection of two critical lines.*

and that the trajectories are not parallel to either critical line. Denoting values at the pseudo-critical point by subscript 0, distance from that point by ρ and differentiation along the trajectory by d/ds, we find, using (A.5)

$$dG/ds = (G_0'/F_0')\, dF/ds + \delta,$$

where δ is of the third order in ρ, whereas in general the difference between grad G and a constant times grad F is at least of the first order in ρ (second order in ρ if $F_{x0} = F_{y0} = G_{x0} = G_{y0} = 0$). A typical plot of the variation in F and G along a trajectory traversing the two critical lines near the pseudo-critical point is given in Fig. 7b. (Geometrically, dF/ds approximates a hyperbolic paraboloid—such as $dF/ds \propto xy$—with its saddle point at the pseudo-critical point and its horizontal generatrices along the critical lines.) Thus, to a high order of approximation, jumps will occur between points on the same trajectory. In the first approximation, the length of the jump is 1.5 times the distance between the critical lines measured along the trajectory. Obviously, we cannot say that this jump must be unique, but in a physical application it presumably would be.

When studying non-linear systems, it is essential to keep the physical background in mind. When a system is assumed to be stationary in time, the assumption may have to be tested experimentally. The justification of the discontinuity treatment of critical points is empirical and the same must be true regarding pseudo-singular and pseudo-critical points. As an example where pseudo-singular points occur in an initial-value problem we may choose the Abraham-Bloch multivibrator. (See e.g., Minorsky, *loc. cit.* Sec. 137.) Using the two grid voltages as phase variables, we can describe the situation thus. For vibrations to be possible, the characteristic parameter $f_{max} = rRS_{max}/(R + r)$ must exceed unity. When f_{max} is slightly greater than one we expect a pseudo-nodal point in the first quadrant with a smooth transition towards the origin and when f_{max} is somewhat greater we expect a pseudo-nodal point with its slope of approach approximately parallel to the critical line. Finally, when f_{max} is still greater, this point corresponds to a pseudo-saddle point with a pseudo-focal point on each side.